We are IntechOpen, the world's leading publisher of Open Access books Built by scientists, for scientists

4,800
Open access books available

122,000
International authors and editors

135M
Downloads

Our authors are among the

154
Countries delivered to

TOP 1%
most cited scientists

12.2%
Contributors from top 500 universities

CLARIVATE ANALYTICS BOOK CITATION INDEX INDEXED

WEB OF SCIENCE™

Selection of our books indexed in the Book Citation Index in Web of Science™ Core Collection (BKCI)

Interested in publishing with us?
Contact book.department@intechopen.com

Numbers displayed above are based on latest data collected.
For more information visit www.intechopen.com

10

Wavelet Transform in Fault Diagnosis of Analogue Electronic Circuits

Lukas Chruszczyk
Silesian University of Technology
Poland

1. Introduction

The aim of the chapter is description of a wavelet transform utilisation in fault diagnosis of analogue electronic circuits. The wavelet transform plays a key role in the presented methods and is located in important step of a feature extraction.

The chapter, among wavelet transform, contains also applications of other modern computational technique: evolutionary optimisation on example of a genetic algorithm, which has proven to be robust and effective optimisation tool for this kind of problems (Bernier et al. 1995; Goldberg, 1989; Grefenstette, 1981, 1986; Holland 1968; De Jong, 1975, 1980; Pettey et al., 1987; Suh & Gucht, 1987; Tanese, 1987).

The author's intention is presentation of a practical utilisation of abovementioned methods (and their combination) in field of testing (fault diagnosis) of analogue electronic circuits.

2. Fault diagnosis of analogue electronic circuits

An electrical and electronic circuit testing is an inseparable part of manufacturing process. Depending on circuit type (analogue, digital, mixed), function (amplifier, oscillator, filter, mixer, nonlinear etc.) and implementation (tube or semiconductor, discrete, integrated) there have been proposed variety of testing methods. Together with development of modern electronic circuits, test engineers face more and more difficult problems related with testing procedures. Common problems are constant grow of complexity, density, functionality, speed and precision of circuits. At the same time contradictory factors like time-to-market, manufacturing and testing cost must be minimised while testing speed maximised. Important problem is also limited access to internal nodes of integrated circuits. All these problems are related to any "life epoch" of electronic circuit: from design itself, through design validation, prototype characterisation, manufacturing, post-production test (quality control) and finally board/field testing (Huertas, 1993). It must be noted: the later a fault is detected, the faster grows related cost. While final functional testing is unavoidable, there is still an effort in finding fast and simple methods detecting at least the most probable faults in early life stage of a circuit.

The proposed description of testing methods is limited to fault diagnosis of analogue electronic circuits (AEC). Testing of such circuits meets specific problems (i.e. components tolerance, fault masking, measurement inaccuracy) not presented in testing other circuits

types (e.g. digital). Utilisation of a wavelet transform can greatly improve efficiency of selected fault diagnosis and, in some cases, makes the diagnosis feasible at all. The wavelet transform is used here as a feature extraction procedure. It must be noted that despite of dominant role of a digital and microprocessor electronic devices, there will never be escape from analogue circuits. Growing complexity of analogue and mixed-level electronic systems (e.g. system-on-chip – SoC) still rises the bar for testing methods (Baker et al., 1996; Balivada et al., 1996; Chruszczyk et al. 2006, 2007; Chruszczyk & Rutkowski 2008, 2009, 2011; Chruszczyk 2011; Dali & Souders 1989; Kilic & Zwolinski, 1999; Milne et al., 1997; Milor & Sangiovanni-Vincentelli, 1994; Pecenka et al., 2008; Saab et al. 2001; Savir & Guo, 2003; Somayajula et al., 1996).

2.1 Test environment

There have been taken following assumptions on the test procedure:

1. the only available test nodes of a circuit under test (CUT) are the external nodes,
2. CUT is excited by aperiodic excitation and its shape is optimised for given circuit,
3. the only available information about CUT state is read from measurement of four quantities (fig. 1):
   a. output voltage $y_1(t)$,
   b. input current $y_2(t)$,
   c. supply currents $y_3(t)$ and $y_4(t)$.

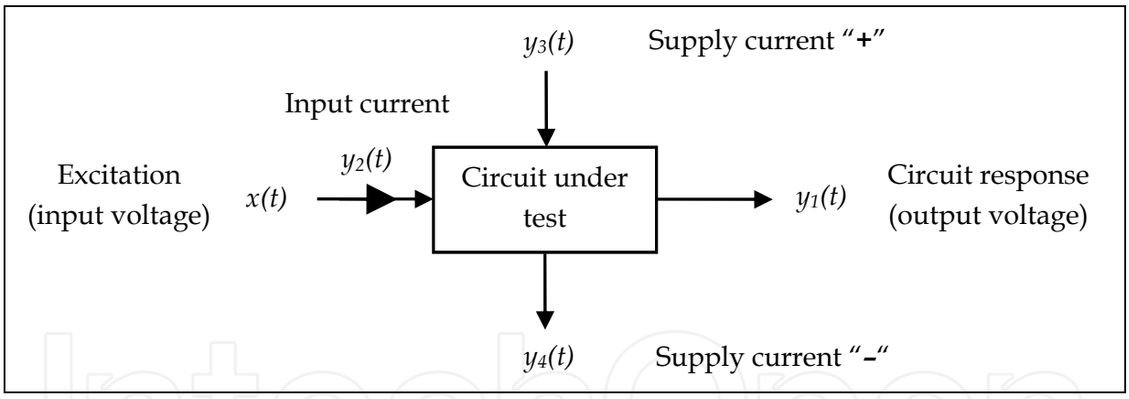

Fig. 1. Assumed test procedure

There are only measured output voltage $y_1(t)$ and input current $y_2(t)$ in case of a passive circuits.

The optimisation goal is the best shape of input excitation voltage (in time-domain). Generally, it can be described as a continuous time function x(t) (fig. 2):

$$x(t) \in \mathbb{R}; \quad t \in [0, t_{max}] \tag{1}$$

Due to practical reasons, there has been assumed discrete form of excitation x(n) described by sequence of N_P samples x_n with constant sampling period T_s. The sampling period always conforms Whittaker-Nyquist-Kotelnikov-Shannon sampling theorem for excitation x(t) and all measured CUT responses. Additionally, value of T_s is set to be 10 times smaller

than the smallest time constant of a linear CUT. This ensures good approximation of a continuous excitation x(t) by its discrete equivalent. Maximal time length t_{max} of excitation x(t) (so its discrete approximation x(n) as well) is set to be 5 times greater than the longest time constant of a linear CUT. Value of each sample x_n is quantised to *K* levels (fig. 3):

$$\{x(t_1), x(t_2), x(t_3), \dots\} \in x(t) \tag{2}$$

$$\begin{gathered} x_n = x(t_n) \\ t_{n+1} - t_n = T_s = const\,; \quad n = 1, 2, \dots, N_p \end{gathered} \tag{3}$$

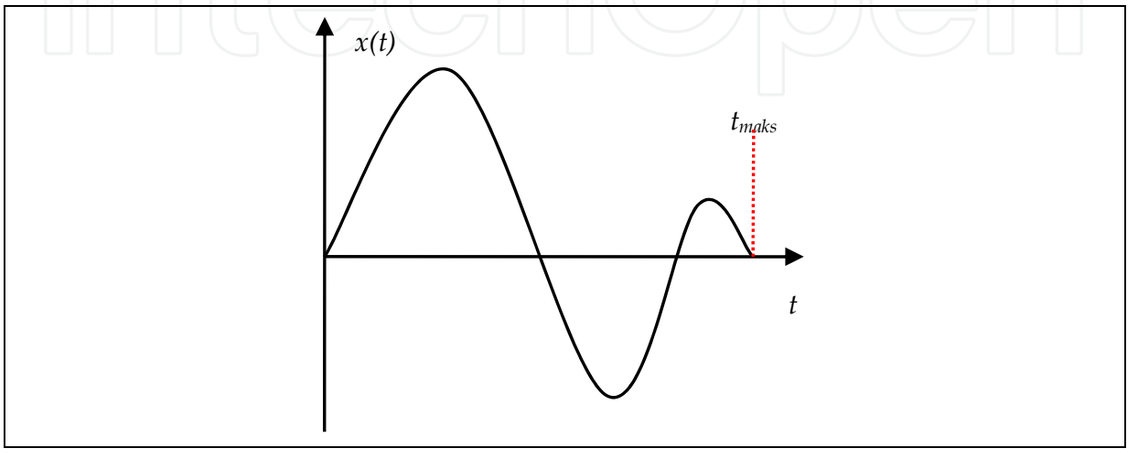

Fig. 2. General form of an input excitation

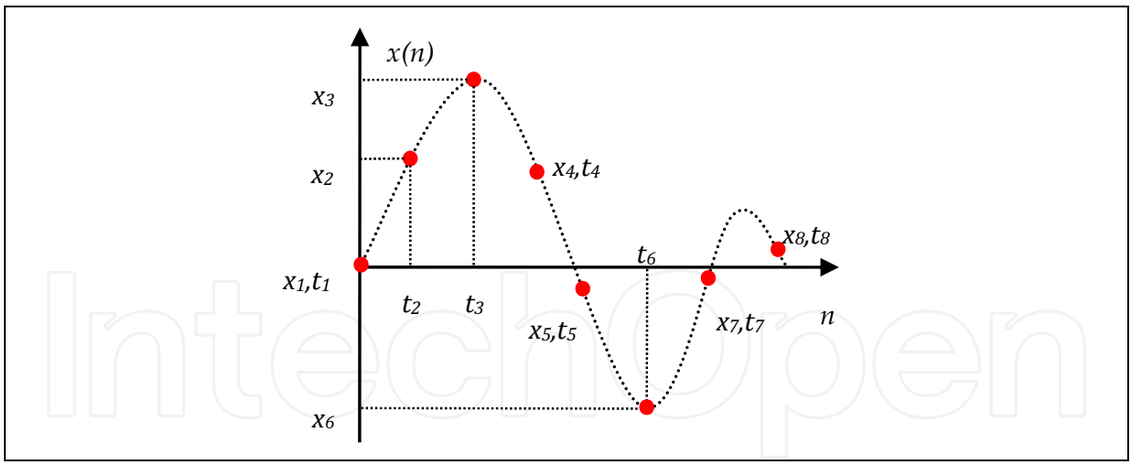

Fig. 3. Input excitation sampling

In order to consider influence of real digital-to-analogue (A/D) converters, there have been used two types of x(n) approximations:

1. "step-shape" (0th-order polynomial), fig. 4,
2. piece-wise linear (1st-order polynomial), fig. 5.

There have been analysed only single catastrophic (hard) and parametric (soft) circuit faults, because such faults are the most probable.

2.2 General tester structure

Fig. 6 presents general tester structure. The tester generates excitation signal and makes decision about CUT state (fault) based on analysis of measured CUT responses.

According to different goals of performed fault diagnosis (detection, location or identification) structure of a diagnostic system is shown on fig. 7. The D–Tester (fault detector) returns on of the following decisions:

- GO – meaning "non-faulty - healthy circuit",
- NO GO – means "faulty circuit" or
- "unknown" if, for any reason, classification cannot be performed.

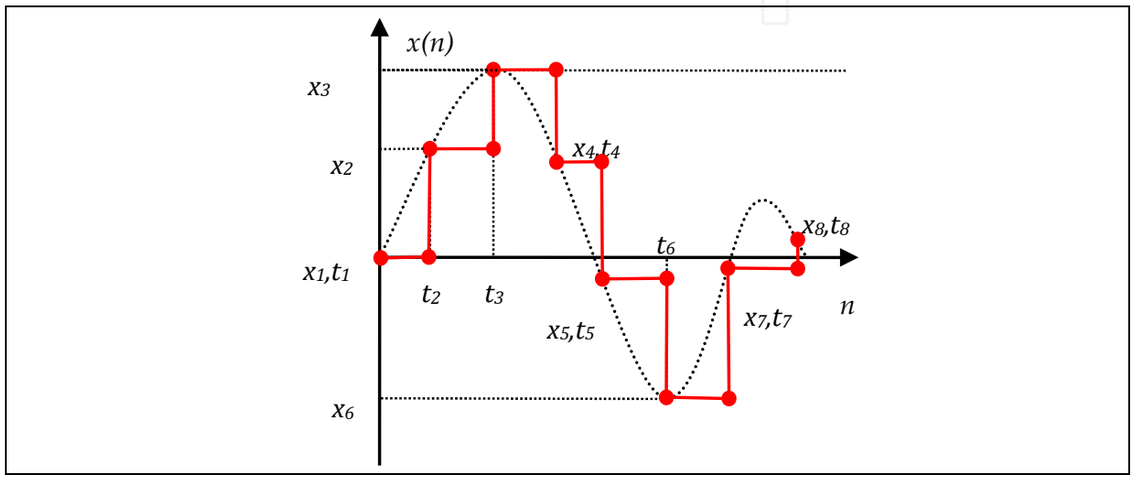

Fig. 4. "Step-shape" (0th-order polynomial) approximation of input excitation

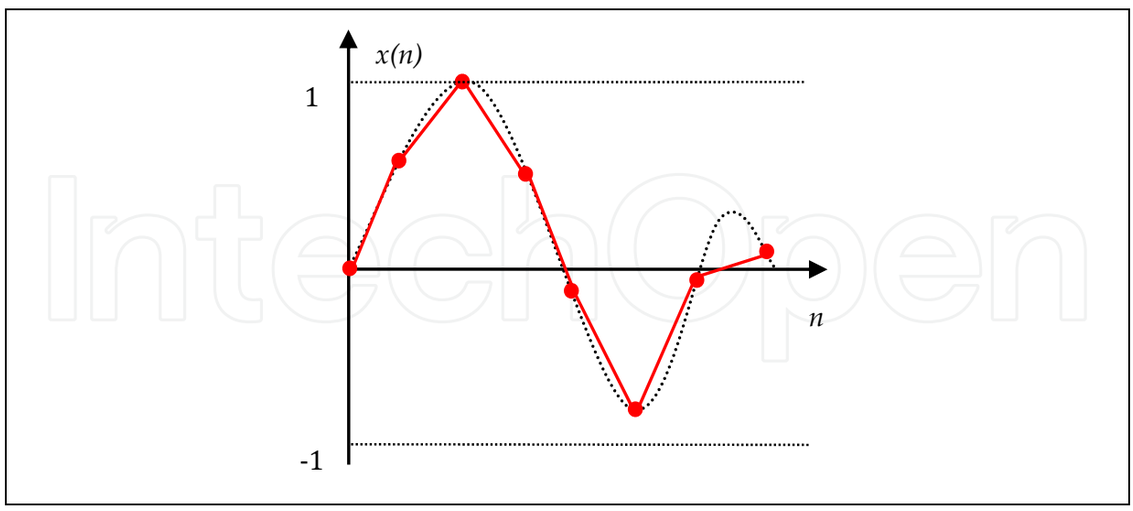

Fig. 5. Piece-wise linear (1st-order polynomial) approximation of input excitation

If fault detection is the only performed diagnosis type, the "unknown" decision can be replaced by NO GO decision (the worst case). This obviously reduces test yield, but does not deteriorates diagnosis trust level.

The L–Tester (fault location) points which circuit element is faulty or decision "?", if proper classification cannot be performed.

The deepest level: fault identification (information about faulty element value or at least its shift – represented by I–Tester) has not been analysed in this work.

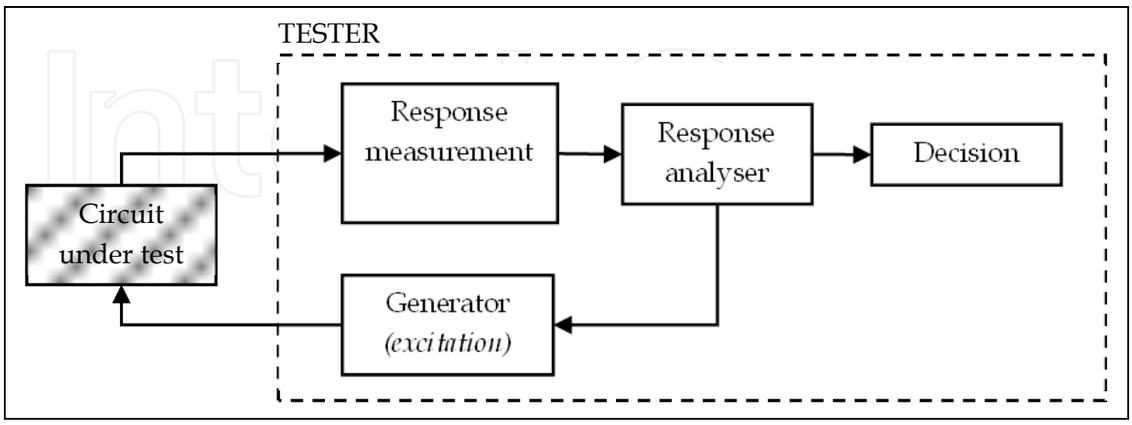

Fig. 6. General tester structure

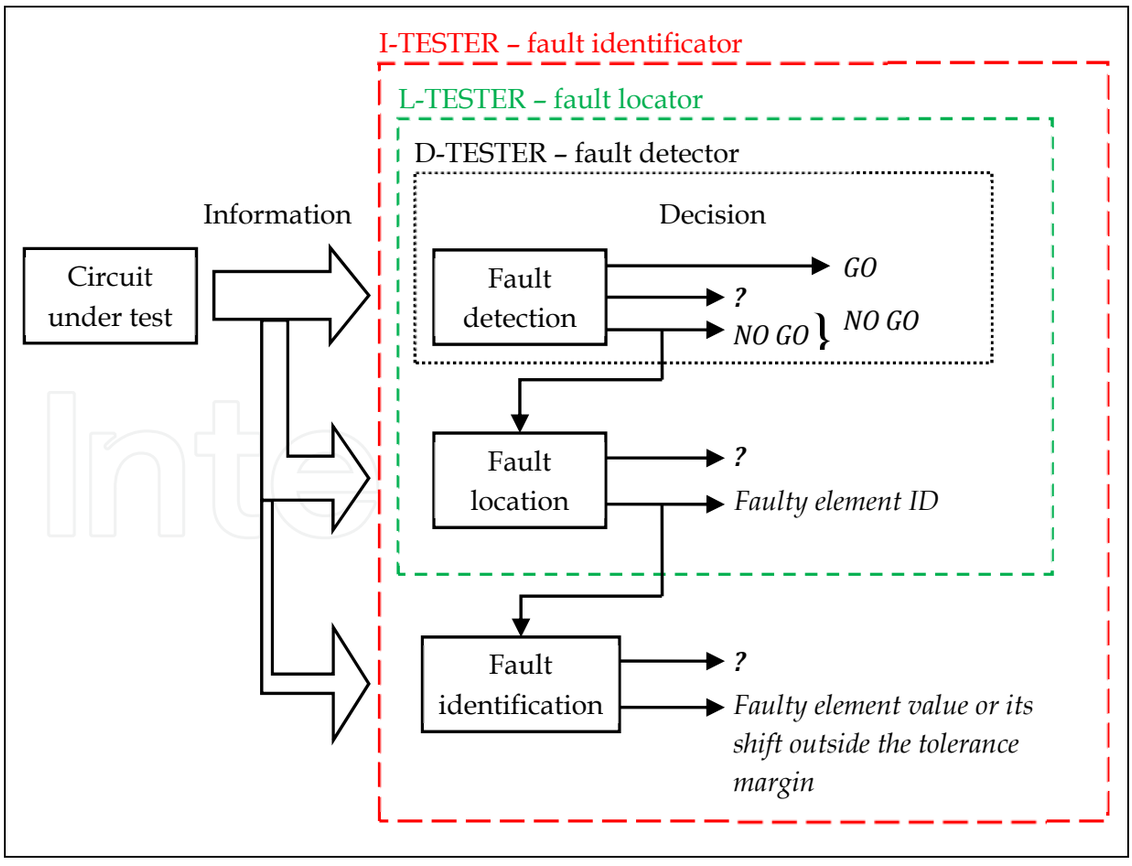

Fig. 7. Fault diagnosis levels

2.3 Fault detection: D-Tester design

Presented fault diagnosis method belongs to class SBT (Simulate-Before-Test) with *fault dictionary*. The dictionary contains information related to selected faults that are simulated *before* circuit measurements. There is defined set **F** containing selected N_F faults F_k, k = 1, 2, …, N_F. Fault numbered 0 (F_0) is used to code healthy (non-faulty) circuit:

$$\boldsymbol{F} = \{F_0, F_1, F_2, \ldots, F_{NF}\} \tag{4}$$

Figure below presents structure of the D-Tester (fault detector).

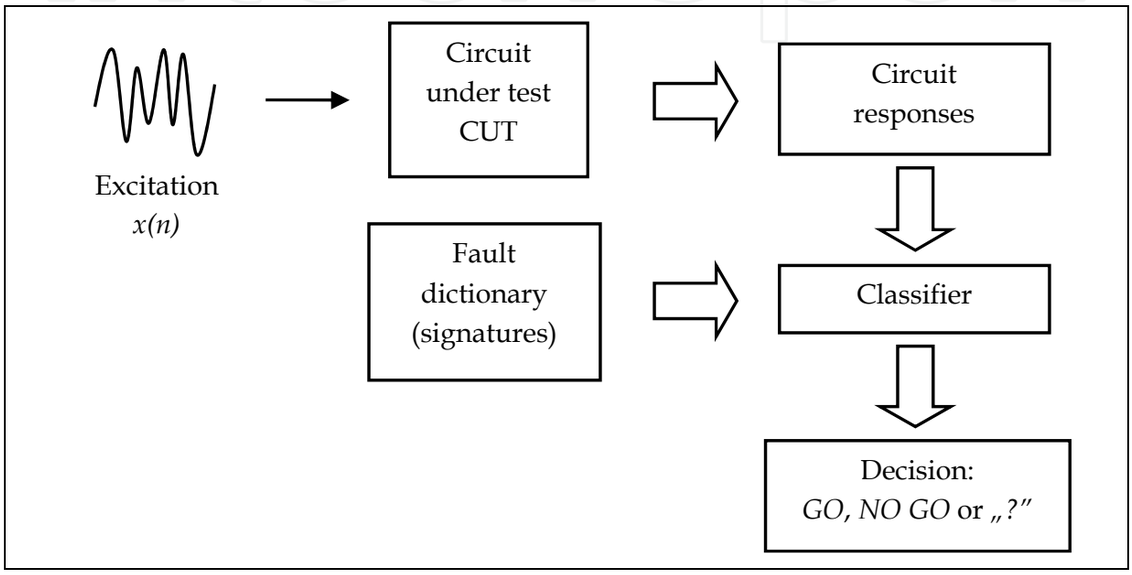

Fig. 8. D-Tester (fault detector) structure

The fault dictionary **S** is built from simulated CUT responses (for all analysed faults). The dictionary contains N_F + 1 fault signatures S_k, k = 0, 1, 2…, N_F, where each signature S_k corresponds to fault F_k (fig. 9).

The example of the fault dictionary for single response y(n) is placed below:

$$\mathbb{S} = \{S_0, S_1, \ldots, S_{NF}\} = \begin{bmatrix} S_0 \\ S_1 \\ \ldots \\ S_{NF} \end{bmatrix} \tag{5}$$

Each particular signature S_k is vector containing samples of response y(n) = { y_1, y_2, …, y_{Np} }:

$$\mathbb{S} = \begin{bmatrix} S_0 \\ S_1 \\ \ldots \\ S_{NF} \end{bmatrix} = \begin{bmatrix} y^{S_0}(n) \\ y^{S_1}(n) \\ \ldots \\ y^{S_{NF}}(n) \end{bmatrix} = \begin{bmatrix} y_1^{S_0} & y_2^{S_0} & \ldots & y_{N_P}^{S_0} \\ y_1^{S_1} & y_2^{S_1} & \ldots & y_{N_P}^{S_1} \\ \ldots & \ldots & \ldots & \ldots \\ y_1^{S_{NF}} & y_2^{S_{NF}} & \ldots & y_{N_P}^{S_{NF}} \end{bmatrix} \tag{6}$$

so, each signature can represented by discrete series of samples:

$$S_k = y^{S_k}(n) = s_k(n) = \left\{s_1, s_2, \ldots, s_{N_p}\right\}_k; \quad k = 0, 1, \ldots, N_F \tag{7}$$

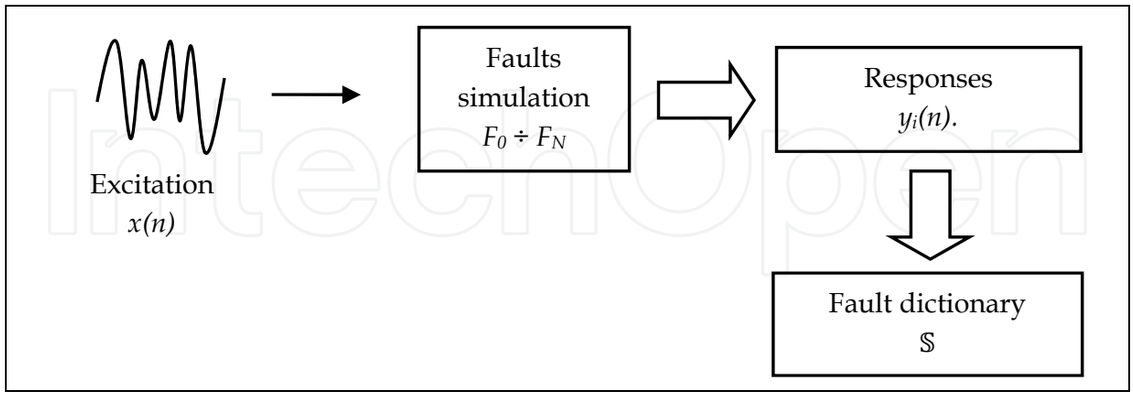

Fig. 9. Schema of fault dictionary creation

According to the test and measurement assumptions, excited passive CUT returns two responses: output voltage $y_1(n)$ and input current $y_2(n)$, where excited active CUT returns four responses - additionally positive $y_3(n)$ and negative supply current $y_4(n)$. The dictionary **S** contains fault signatures $S_{i,k}$, k = 0, 1, 2…, N_F for particular CUT responses $y_i(n)$. Example for passive CUT is presented on fig. 10 (i = 1, 2):

$$\mathbb{S} = \begin{bmatrix}\mathbb{S}\{y_1(n)\}\\ \mathbb{S}\{y_2(n)\}\end{bmatrix} = \begin{bmatrix} S_{y_1(n),0}\\ S_{y_1(n),1}\\ \ldots\\ S_{y_1(n),NF}\\ S_{y_2(n),0}\\ S_{y_2(n),1}\\ \ldots\\ S_{y_2(n),NF}\end{bmatrix} = \begin{bmatrix} y_1^{S_0}(n)\\ y_1^{S_1}(n)\\ \ldots\\ y_1^{S_{NF}}(n)\\ y_2^{S_0}(n)\\ y_2^{S_1}(n)\\ \ldots\\ y_2^{S_{NF}}(n)\end{bmatrix} \tag{8}$$

Tolerances of circuit elements must be taken into consideration when building fault dictionary. There has been used Monte-Carlo (MC) function of a PSpice simulator. Values of non-faulty elements are uniformly random within their tolerance interval. The result is multiplication of CUT responses, thus fault signatures, by factor N_{MC} + 1, where N_{MC} is number of performed Monte-Carlo analyses (without nominal circuit). The example below is a fault dictionary for passive CUT (i = 1, 2) and two Monte-Carlo analyses (m = 0, 1, 2), where m = 0 = „nom" denotes circuit with nominal values of elements:

$$\mathbb{S} = \begin{bmatrix}\mathbb{S}\{y_1(n)\}\\ \mathbb{S}\{y_2(n)\}\end{bmatrix} \xrightarrow{MC\ analysis} \mathbb{S}' = \begin{bmatrix} \mathbb{S}\{y_1(n)\}_{MC="nom"}\\ \mathbb{S}\{y_1(n)\}_{MC=1}\\ \mathbb{S}\{y_1(n)\}_{MC=2}\\ \mathbb{S}\{y_2(n)\}_{MC="nom"}\\ \mathbb{S}\{y_2(n)\}_{MC=1}\\ \mathbb{S}\{y_2(n)\}_{MC=2}\end{bmatrix} \tag{9}$$

$\mathbf{S_{i,k}}$ means set of signatures of k-th fault for i-th response $y_i(n)$, obtained from N_{MC} Monte-Carlo simulation, where k = 0, 1, 2, …, N_F and i = 1, 2 for passive or i = 1, 2, 3, 4 for active circuit:

$$\boldsymbol{S_{i,k}} = \begin{bmatrix} S_{k,MC="nom"} \\ S_{k,MC=1} \\ S_{k,MC=2} \end{bmatrix}; \quad k = 0, 1, \dots, N_F \tag{10}$$

Totally, the fault dictionary for passive CUT contains $2\cdot(N_{MC}+1)\cdot(N_F+1)$ signatures and for active CUT: $4\cdot(N_{MC}+1)\cdot(N_F+1)$ signatures.

Figure 10 contains exemplary signatures for single CUT response and two selected faults F_1 and F_2. Number of Monte-Carlo analyses is N_{MC} = 4. There has been assumed that location of particular signature is distance from signature S_0^{nom} (healthy nominal circuit). If there are no Monte-Carlo analysis performed (all circuits are nominal), the horizontal axis contains only S_i^m signatures. The Monte-Carlo analysis introduces spread around nominal values and single signatures turn into a group of signatures $S_{i,k}^m$, where m = 1, 2, …, N_{MC} for i-th CUT response $y_i(n)$ and k-th fault F_k. This enables finding border values of the signature sets (groups) – fig. 10.

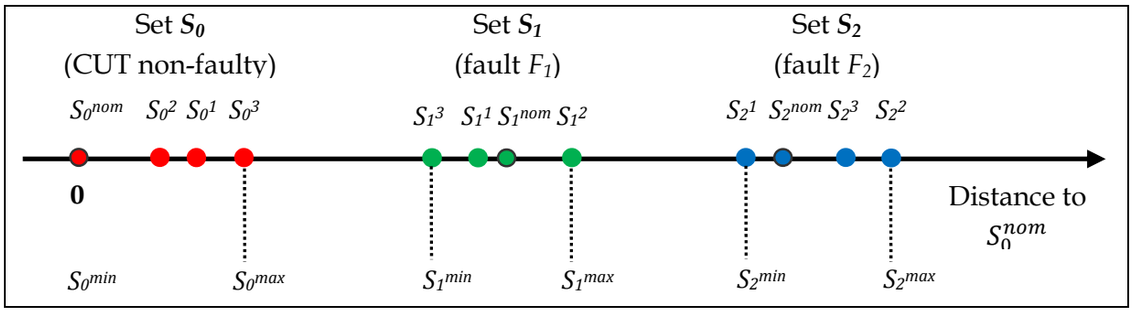

Fig. 10. Example of signature sets (groups) for single response and N_F = 2, N_{MC} = 4

Distance of each circuit response $y_i(n) = \{y_1, y_2, \dots y_n, \dots, y_{N_P}\}_i$ from appropriate fault signature $\boldsymbol{S_{i,k}} = S_{i,k}^m = s_{i,k}^m(n) = \{s_1, s_2, \dots, s_n, \dots, s_{N_p}\}_{i,k}^m$ has been calculated in two alternative ways:

1. one-dimensional Euclidean distance d:

$$d^i(k,m) = \sqrt{\sum_{n=1}^{N_p} \left[y_n^i - s_{i,k,n}^m\right]^2} \qquad \begin{matrix} k = 0, 1, \dots, N_F \\ m = 0, 1, \dots, N_{MC} \end{matrix} \tag{11}$$

where: i = 1, 2 for passive CUT or i = 1, 2, 3, 4 for active one,

2. absolute difference d and selected threshold U_{min}:

$$r^i(k,m) = \begin{cases} 1 & if \quad \left|y_n^i - s_{i,k,n}^m\right| > U_{min} \\ 0 & elsewhere \end{cases}; \quad \begin{matrix} k = 0, 1, \dots, N_F \\ m = 0, 1, \dots, N_{MC} \end{matrix} \tag{12}$$

$$d^i(k,m) = \sum_{m=0}^{N_{MC}} \sum_{k=0}^{N_F} r^i(k,m) \tag{13}$$

where: i = 1, 2 for passive CUT or i = 1, 2, 3, 4 for active CUT. Level of the threshold U_{min} is related to measurement accuracy and is chosen arbitrarily by test engineer.

2.4 Fault location: L-Tester design

According to fig. 7, step of the fault location is performed only, if fault detector returns decision NO GO. Then, fault locator tries to find which element is responsible for circuit fault or returns decision "?" ("unknown"). The structure, design and work of L-Tester is similar to the D-Tester, except missing state F_0 (healthy circuit) in set **F** of analysed circuit faults. It must be noted that, despite of one CUT state less to classify from (F_0), the diagnosis goal of fault location is much more difficult than fault detection.

Totally, the fault dictionary contains $2\cdot(N_{MC}+1)\cdot N_F$ signatures for passive circuit or $4\cdot(N_{MC}+1)\cdot N_F$ signatures for active CUT.

3. Utilisation of a wavelet transform

One of alternative methods for simultaneous time-frequency analysis is a wavelet transform (Daubechies, 1992). The most important differences comparing to popular Fourier transform are:

- use of base function with limited (or approximately limited) time domain. This implies that base function must be *aperiodic*,
- base function is *scaled* and *shifted* simultaneously.

Conceptually wavelet transform is equivalent to constant percentage bandwidth frequency analysis: $\Delta f/f0=const$, used. e.g. in acoustics, but differently implemented.

The formula below defines continuous real wavelet transform (Daubechies, 1992):

$$X(a,b) = \frac{1}{\sqrt{|a|}} \int_{-\infty}^{\infty} x(t)\, \psi\left(\frac{t-b}{a}\right) dt \;; \qquad a \neq 0; \quad a, b \in \mathbb{R} \tag{14}$$

The function ψ(t) is called base wavelet (or mother wavelet) and its stretched and shifted form $\psi_{a,b}(t)$ called just a wavelet:

$$\psi_{a,b}(t) = \psi\left(\frac{t-b}{a}\right); \qquad a \neq 0; \quad a, b \in \mathbb{R} \tag{15}$$

The parameter *a* (called *scale* parameter) is responsible for analysis "resolution". Small value corresponds to high detail level which can be analysed in function x(t). This is analogue to high frequency harmonics in Fourier transform. The parameter *b* (*shift*) is responsible for location on the time axis (fig. 11).

The inverse transform is defined as (Daubechies, 1992):

$$x(t) = \int_0^{\infty} \int_{-\infty}^{\infty} \frac{1}{a^2} X(a,b) \frac{1}{\sqrt{|a|}} \varphi\left(\frac{t-b}{a}\right) db\, da \tag{16}$$

where φ is a synthesising function, dual to the analysing wavelet function ψ and satisfying condition:

$$\int_0^{\infty}\int_{-\infty}^{\infty}\frac{1}{|a^3|}\varphi\left(\frac{t_1-b}{a}\right)\varphi\left(\frac{t-b}{a}\right)\,db\,da=\delta(t_1-t) \tag{17}$$

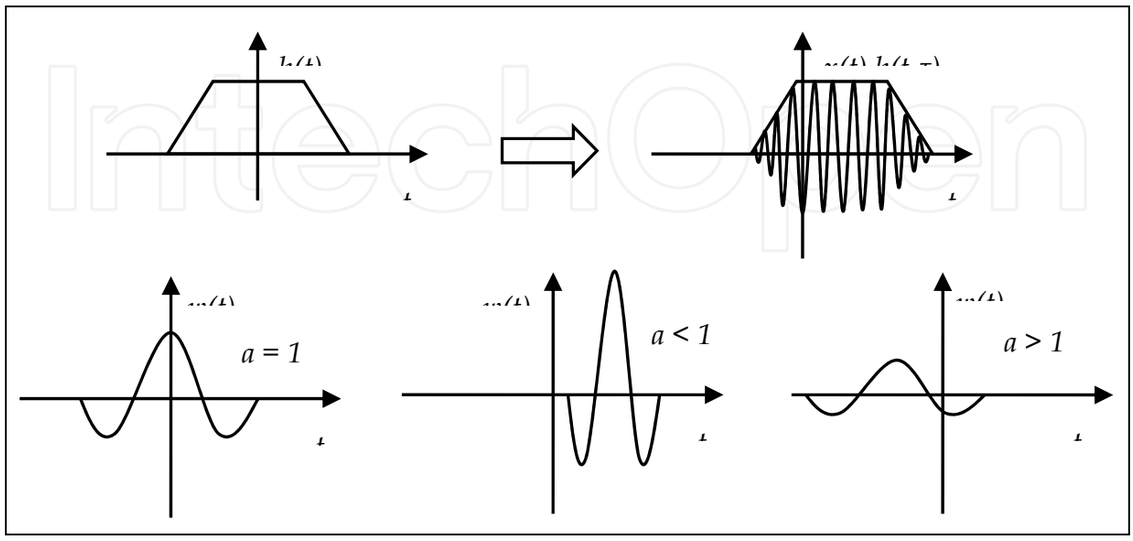

Fig. 11. Scaling and shifting of the base functions in short-time Fourier transform (STFT) and in wavelet transform

3.1 Discrete wavelet transform

In case of a discrete function x(n), the parameters of scale *a* and shift *b* are discrete as well and equation (14) is modified:

$$X(m,n)=a_0^{-\frac{m}{2}}\int_{-\infty}^{\infty}x(t)\,\psi(a_0^{-m}\,t-n\,b_0)\,dt \tag{18}$$

In order to completely, but non redundantly cover domain of analysed function x(n), the parameters *a* and *b* must be calculated as follows (Daubechies, 1992):

$$a=a_0^m;\quad b=nb_0a_0^m;\quad m,n\in\mathbb{C};\ a_0>1;\ b_0>0 \tag{19}$$

Unfortunately, in case of a discrete wavelet transform, there is no guarantee of reconstruction of x(n) based only on values of X(m,n) coefficients (Daubechies, 1992).

3.2 Applied modifications of a wavelet transform

Utilisation of a wavelet transform as a feature extractor is based on a continuous transform. Numerical calculations (performed in Matlab environment) lead to following assumptions:

- domain of a function x(n) is limited:

$$\text{supp}[\,x(n)]\in[0;t_{max}] \tag{20}$$

- continuous function x(t) is approximated by discrete x(n) (0^{th} order polynomial, fig. 4),

- values of scale parameter *a* are limited to natural numbers and value of a_{max} is selected by test engineer:

$$a = 1, 2, \dots, a_{max} \tag{21}$$

- values of shift parameter *b* are limited to natural numbers including 0:

$$b = 0, 1, \dots, N_P - 1 \tag{22}$$

This allows following transformations of formula (14):

$$X(a,b) = \frac{1}{\sqrt{a}} \sum_{n=-\infty}^{\infty} \int_{n}^{n+1} x(t)\, \psi\left(\frac{t-b}{a}\right) dt \tag{23}$$

$$X(a,b) = \frac{1}{\sqrt{a}} \sum_{n=-\infty}^{\infty} x(n) \int_{n}^{n+1} \psi\left(\frac{t-b}{a}\right) dt \tag{24}$$

$$X(a,b) = \frac{1}{\sqrt{a}} \sum_{n=1}^{N_P} x(n) \left(\int_{-\infty}^{n+1} \psi\left(\frac{t-b}{a}\right) dt - \int_{-\infty}^{n} \psi\left(\frac{t-b}{a}\right) dt \right) \tag{25}$$

where expression:

$$\int_{-\infty}^{n} \psi(t) dt \tag{26}$$

is calculated numerically, dependent on selected base wavelet (Daubechies, 1992). In simplified case, when mother wavelet ψ(t) exists in analytical form, equation (25) can be expressed directly in discrete form:

$$X(a,b) = \frac{1}{\sqrt{a}} \sum_{n=1}^{N_P} x(n)\, \psi\left(\frac{n-b}{a}\right); \quad \begin{matrix} a = 1, 2, \dots, a_{max} \\ b = 0, 1, \dots, N_P - 1 \end{matrix} \tag{27}$$

The above formula clearly shows, that there must performed N_P operations of convolution of sequence x(n) with discrete wavelet ψ(n) for each value of scale parameter *a*. This allows easy evaluation of a numerical complexity of such transformation.

3.3 Fault detection with wavelet fault dictionary: DW-Tester

CUT returns discrete responses $y_i(n)$ for applied excitation x(n). According to eq. (25) or (27) there is calculated set of wavelet coefficients $Y_i(a,b)$ for each response $y_i(n)$:

$$Y_i(a,b) = TF[y_i(n)] \tag{28}$$

where i = 1, 2 for passive CUT or i = 1, 2, 3, 4 for active CUT and TF is a transform with selected base wavelet function, according to (25) or (27).

$$\mathbb{Y} = \begin{bmatrix} Y_{11} & Y_{12} & \dots & Y_{1,N_P-1} \\ Y_{21} & Y_{22} & \dots & Y_{2,N_P-1} \\ \dots & \dots & \dots & \dots \\ Y_{a_{max},1} & Y_{a_{max},2} & \dots & Y_{a_{max},N_P-1} \end{bmatrix}_{a_{max} \times N_P - 1} \tag{29}$$

Distance of a single CUT response $y_i(n)$ (represented by matrix of wavelet coefficients Y_i) to appropriate fault signature (also in form of a wavelet coefficients $S_k^{F,i,j}$) is calculated as:

1. two-dimensional Euclidean distance:

$$d^i(j,k) = \sqrt{\sum_{a=1}^{a_{max}} \sum_{b=0}^{N_p-1} \left[Y^i(a,b) - S_k^{F,i,j}(a,b)\right]^2} \qquad \begin{matrix} k = 0,1,\dots,N_F \\ j = 1,2,\dots,N_{MC} \end{matrix} \tag{30}$$

where i = 1, 2 for passive CUT or i = 1, 2, 3, 4 for active CUT;

2. two-dimensional linear Pearson correlation:

$$d_P^i = \frac{\sum_{a=1}^{a_{max}} \sum_{b=0}^{N_P-1} \left[Y^i(a,b) - \overline{Y^i}\right]\left[S_k^{F,i,j}(a,b) - \overline{S_k^{F,i,j}}\right]}{\sqrt{\sum_{a=1}^{a_{max}} \sum_{b=0}^{N_P-1} \left[Y^i(a,b) - \overline{Y^i}\right]^2} \sqrt{\sum_{a=1}^{a_{max}} \sum_{b=0}^{N_P-1} \left[S_k^{F,i,j}(a,b) - \overline{S_k^{F,i,j}}\right]^2}} \tag{31}$$

where:

$$\overline{Y^i} = \frac{1}{a_{maks} \cdot (N_P - 1)} \sum_{a=1}^{a_{maks}} \sum_{b=0}^{N_P-1} Y^i(a,b) \tag{32}$$

and:

$$\overline{S_k^{F,i,j}} = \frac{1}{a_{maks} \cdot (N_P - 1)} \sum_{a=1}^{a_{maks}} \sum_{b=0}^{N_P-1} S_k^{F,i,j}(a,b) \tag{33}$$

for:

$$k = 0,1,\dots,N_F \qquad j = 1,2,\dots,N_{MC}$$

where:
i = 1, 2 for passive CUT or i = 1, 2, 3, 4 for active CUT,
$\bar{Y}$ and $\bar{S}$ are mean values of elements of respectively matrixes Y and S,
$S_k^{F,i,j}$ denotes wavelet signature (matrix of wavelet coefficients) of i-th response $y_i(n)$, for k-th fault F_k and j-th Monte-Carlo analysis.

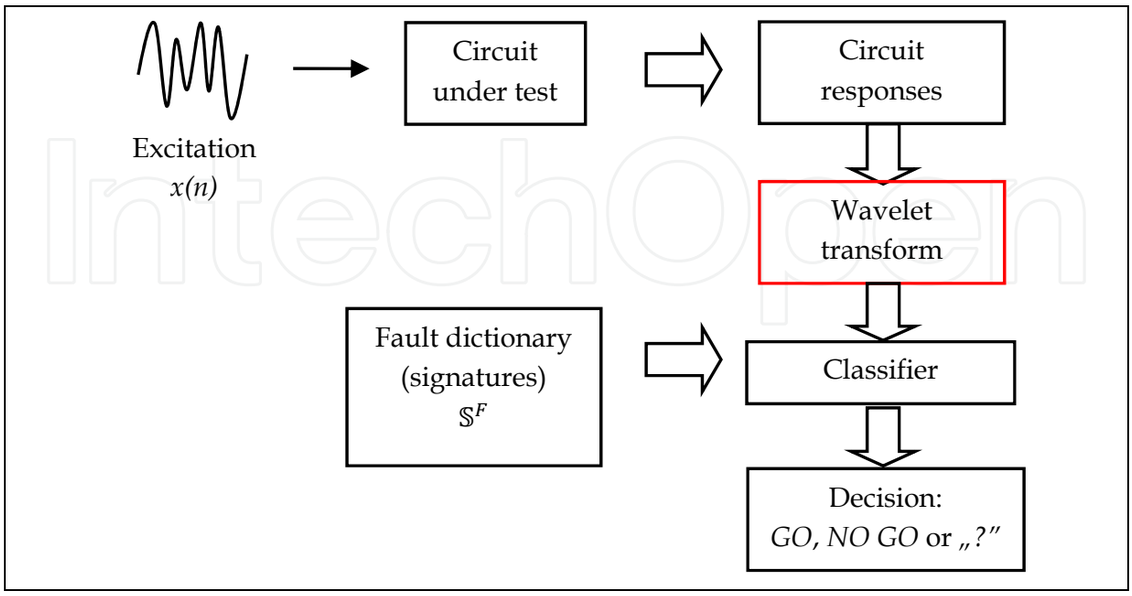

Fig. 12. Schematic of a DW-Tester

3.4 Fault location with wavelet fault dictionary (LW-Tester)

According to fig. 7, the fault location is performed only, if fault detector returns decision NO GO. Then, the fault locator points damaged element or returns decision: "?" ("unknown"). The structure, design and work of LW-Tester is similar to the DW-Tester, except missing state F_0 (healthy circuit) in set **F** of analysed circuit faults.

Distance of a single CUT response $y_i(n)$ (represented by matrix of wavelet coefficients Y_i) from appropriate fault signature (also in form of a wavelet coefficients $S_k^{F,i,j}$) is calculated as follows:

1. two-dimensional Euclid distance:

$$d^i(j,k) = \sqrt{\sum_{a=1}^{a_{max}} \sum_{b=0}^{N_p-1} \left[Y^i(a,b) - S_k^{F,i,j}(a,b)\right]^2} \qquad \begin{matrix} k = 1,2,\dots,N_F \\ j = 1,2,\dots,N_{MC} \end{matrix} \tag{34}$$

where i = 1, 2 for passive CUT or i = 1, 2, 3, 4 for active CUT;

2. two-dimensional linear Pearson correlation:

$$d_P^i = \frac{\sum_{a=1}^{a_{max}} \sum_{b=0}^{N_P-1} \left[Y^i(a,b) - \overline{Y^i}\right]\left[S_k^{F,i,j}(a,b) - \overline{S_k^{F,i,J}}\right]}{\sqrt{\sum_{a=1}^{a_{max}} \sum_{b=0}^{N_P-1} \left[Y^i(a,b) - \overline{Y^i}\right]^2} \sqrt{\sum_{a=1}^{a_{max}} \sum_{b=0}^{N_P-1} \left[S_k^{F,i,j}(a,b) - \overline{S_k^{F,i,J}}\right]^2}} \tag{35}$$

where:

$$\overline{Y^i} = \frac{1}{a_{max} \cdot (N_P-1)} \sum_{a=1}^{a_{max}} \sum_{b=0}^{N_P-1} Y^i(a,b) \tag{36}$$

and:

$$\overline{S_k^{F,i,J}} = \frac{1}{a_{max} \cdot (N_P-1)} \sum_{a=1}^{a_{max}} \sum_{b=0}^{N_P-1} S_k^{F,i,j}(a,b) \tag{37}$$

for:

$$k = 1,2,\dots,N_F \qquad j = 1,2,\dots,N_{MC}$$

where:
i = 1, 2 for passive CUT or i = 1, 2, 3, 4 for active CUT,
$\bar{Y}$ and $\bar{S}$ are mean values of elements of respectively matrixes Y and S,
$S_k^{F,i,j}$ denotes wavelet signature (matrix of wavelet coefficients) of i-th response $y_i(n)$, for k-th fault F_k and j-th Monte-Carlo analysis.

4. Examples

4.1 Example 1: Biquadrate active low-pass filter

Fig. 13 presents biquadrate active low-pass filter [Bali96]. Specialised excitation has been found by means of a genetic algorithm and diagnosis efficiency has been compared to case of testing using simple excitation: input voltage step. There have been selected 8 parametric faults among 4 discrete elements: C_1, C_2, R_2 and R_4: ±10% above and below nominal values. Tolerances of non-faulty elements were equal 2% for resistors and 5% for capacitors. Sampling time of discrete excitation and CUT response was equal to T_s = 50 ns.

There have been investigated three cases, different by method of comparison of CUT responses with appropriate fault signatures and utilisation of wavelet transform.

1. The distance between CUT responses and fault signatures is calculated by means of one-dimensional Euclidean distance (11) and wavelet transform is not used. The excitation x(n) and CUT responses $y_i(n)$ were discretised by $N_P = 200$ samples.
2. Fitness value *fit* of a particular solution in a genetic algorithm was modified by energy density in found excitation frequency spectrum. This introduced positive selection "pressure" on solutions (excitations) with lower high frequency components. The first step was calculation of discrete frequency spectrum F(m) of a excitation x(n) [Lyon99]:

$$F(m) = \sum_{n=0}^{N_P-1} x(n) \cdot e^{-j2\pi m\frac{n}{N}} \qquad m = 0, 1, 2, \ldots, N_P - 1 \tag{38}$$

Then, obtained spectrum was divided into two equal intervals: $\left[0, \frac{1}{4T_s}\right)$ and $\left[\frac{1}{4T_s}, \frac{1}{2T_s}\right)$, or equivalently $\left[0, \frac{N_P}{2} - 1\right]$ and $\left[\frac{N_P}{2}, N_P - 1\right]$. In last step, total energy E_i in each *i*-th interval was calculated:

$$E_1 = \sum_{m=0}^{\frac{N_P}{2}-1} |F(m)|^2 \quad oraz \quad E_2 = \sum_{m=\frac{N_P}{2}}^{N_P-1} |F(m)|^2 \tag{39}$$

Finally, value of fitness function *fit* was modified as follows:

$$\begin{aligned} &jeśli\ E_1 > E_2\ to\ fit \rightarrow 2 \cdot fit \\ &jeśli\ E_1 \leq E_2\ to\ fit \rightarrow \frac{1}{2} \cdot fit \end{aligned} \tag{40}$$

3. There has been used wavelet transform to build fault dictionary. The excitation x(n) and CUT responses $y_i(n)$ were approximated by $N_P = 100$ samples.

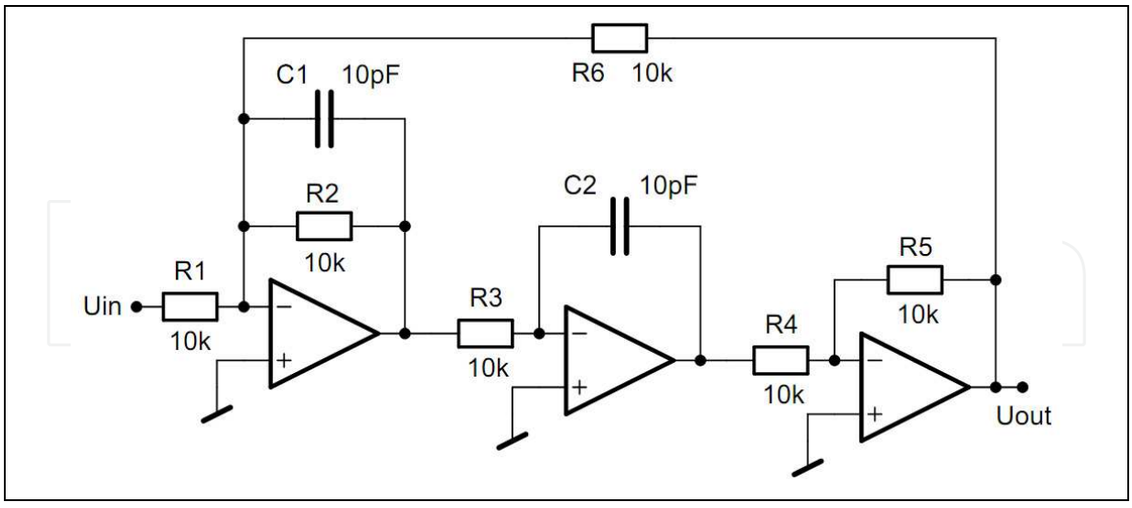

Fig. 13. Biquadrate active low-pass filter [Bali96].

Ad. 1

Figure 14 presents found excitation in time domain and its normalised amplitude spectrum can be found in figure 15. Table 1 shows efficiency of fault detection for step and specialised

excitation (probabilities of a healthy circuit correct detection - true positive H_H; healthy circuit incorrect detection – false negative H_F; faulty circuit correct detection - true negative F_F and faulty circuit incorrect detection - false positive F_H). Similar data, but for case of fault location (probabilities of fault F_x classified as D_x, with correct decisions in main diagonal) can be found in table 2 for found excitation and in table 3 for diagnosis with step excitation.

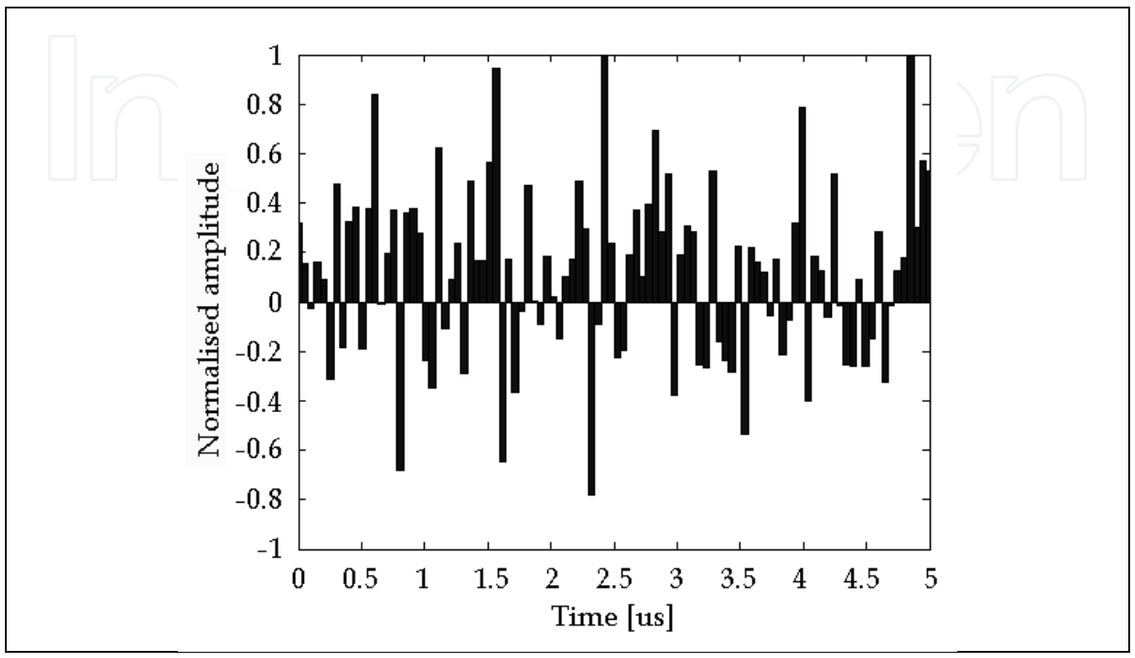

Fig. 14. Found specialised excitation $x_1(n)$

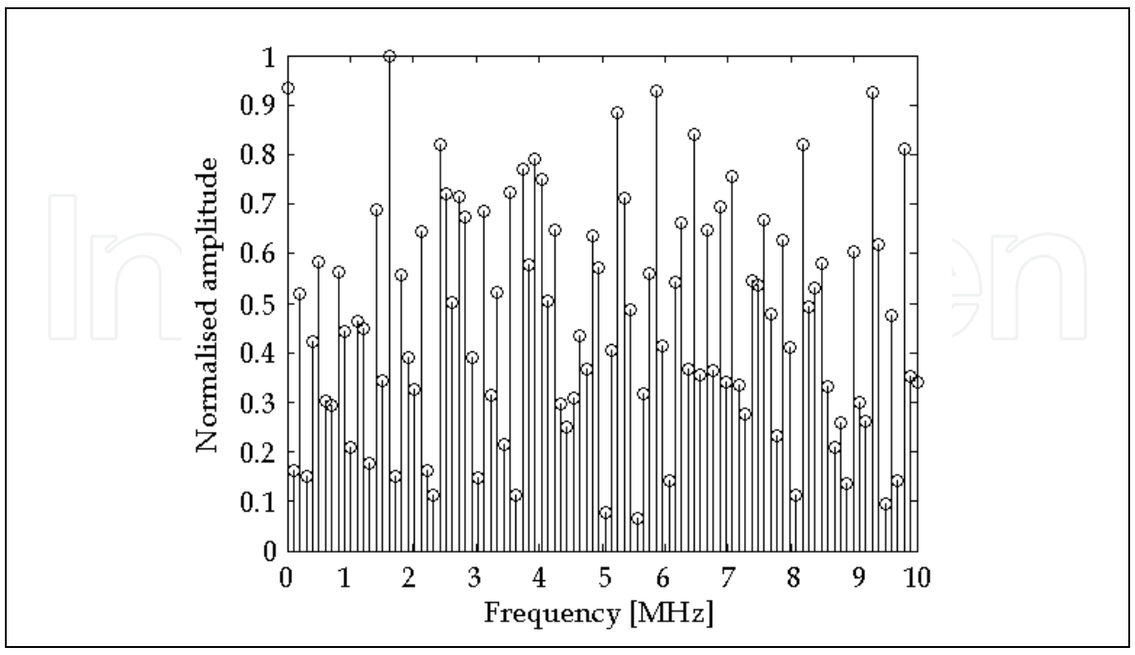

Fig. 15. Normalised frequency (amplitude) spectrum of found excitation $x_1(n)$

Excitation	H_H	H_F	F_F	F_H
$x_1(n)$	0.25	0.75	0.93	0.07
Step	0.03	0.97	0.96	0.04

Table 1. Fault detection efficiency (ad. 1)

	D_1	D_2	D_3	D_4	D_5	D_6	D_7	D_8
F_1	**0.32**	0.02	0.03	0.29	0.03	0	0.27	0
F_2	0.04	**0.36**	0.10	0.01	0	0.05	0	0.17
F_3	0.05	0.23	**0.47**	0	0.04	0	0	0.14
F_4	0.14	0.04	0	**0.43**	0	0.18	0.08	0
F_5	0.01	0	0.14	0	**0.73**	0	0.12	0
F_6	0	0.01	0	0.08	0	**0.71**	0	0.18
F_7	0.17	0	0	0.03	0	0	**0.80**	0
F_8	0	0.19	0.02	0	0	0.05	0	**0.72**

Table 2. Fault location efficiency for specialised excitation (ad. 1)

	D_1	D_2	D_3	D_4	D_5	D_6	D_7	D_8
F_1	**0.14**	0.01	0	0.19	0.29	0.01	0.12	0.22
F_2	0	**0.13**	0.03	0.03	0.37	0.02	0	0.34
F_3	0	0.11	**0.12**	0.04	0.35	0	0	0.34
F_4	0.15	0.02	0	**0.28**	0.20	0.03	0.03	0.21
F_5	0	0	0.06	0.14	**0.41**	0	0.02	0.37
F_6	0.04	0.06	0	0.05	0.21	**0.15**	0	0.37
F_7	0.10	0	0	0.20	0.27	0	**0.27**	0.16
F_8	0	0.21	0.04	0	0.23	0.01	0	**0.49**

Table 3. Fault location efficiency for step excitation (ad. 1)

It can observed that found specialised excitation $x_1(n)$ increased test yield in case of fault detection (tab. 1) and efficiency proper fault location was 1.5 ÷ 5 times greater (tab. 2 and 3 main diagonals, better values marked red).

Ad. 2

Figure 16 presents found excitation in time domain and its normalised amplitude spectrum in figure 17. Table 4 shows efficiency of fault detection for step and specialised excitation (probabilities of a healthy circuit correct detection - true positive H_H; healthy circuit incorrect detection – false negative H_F; faulty circuit correct detection - true negative F_F and faulty circuit incorrect detection - false positive F_H). Similar data, but for case of fault location (probabilities of fault F_x classified as D_x, with correct decisions in main diagonal) can be found in table 5 for designed excitation and in table 6 for diagnosis with step excitation.

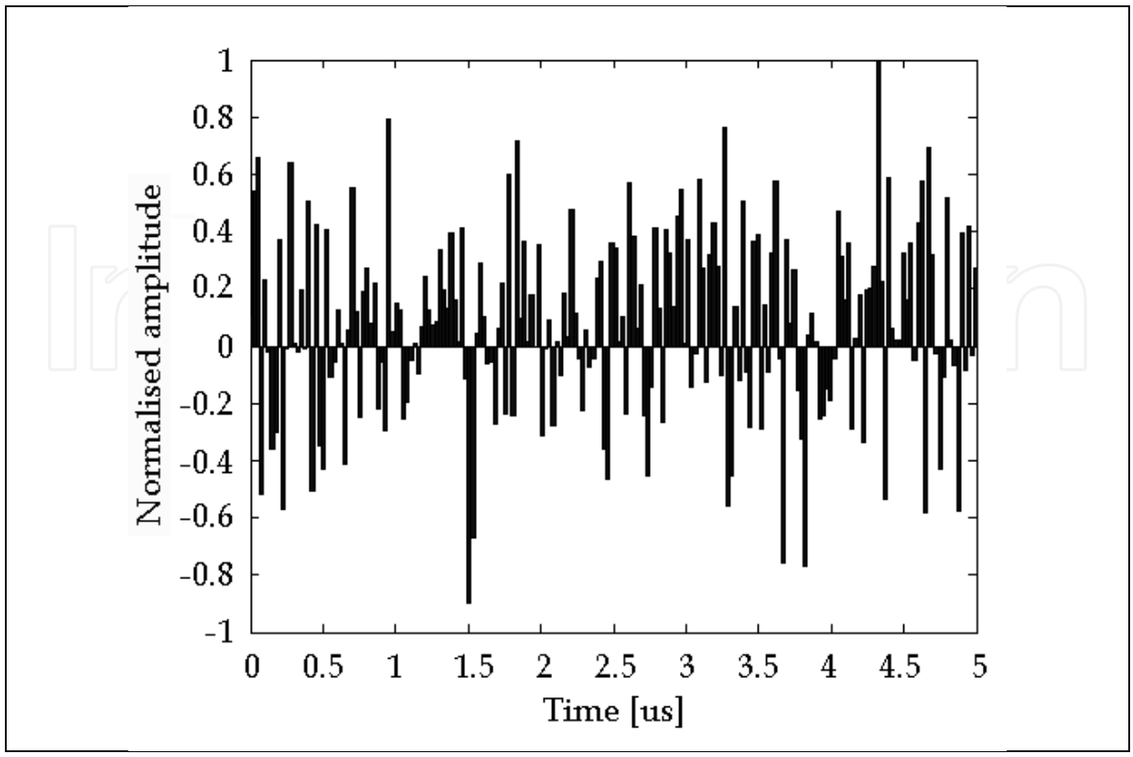

Fig. 16. Found specialised excitation $x_2(n)$

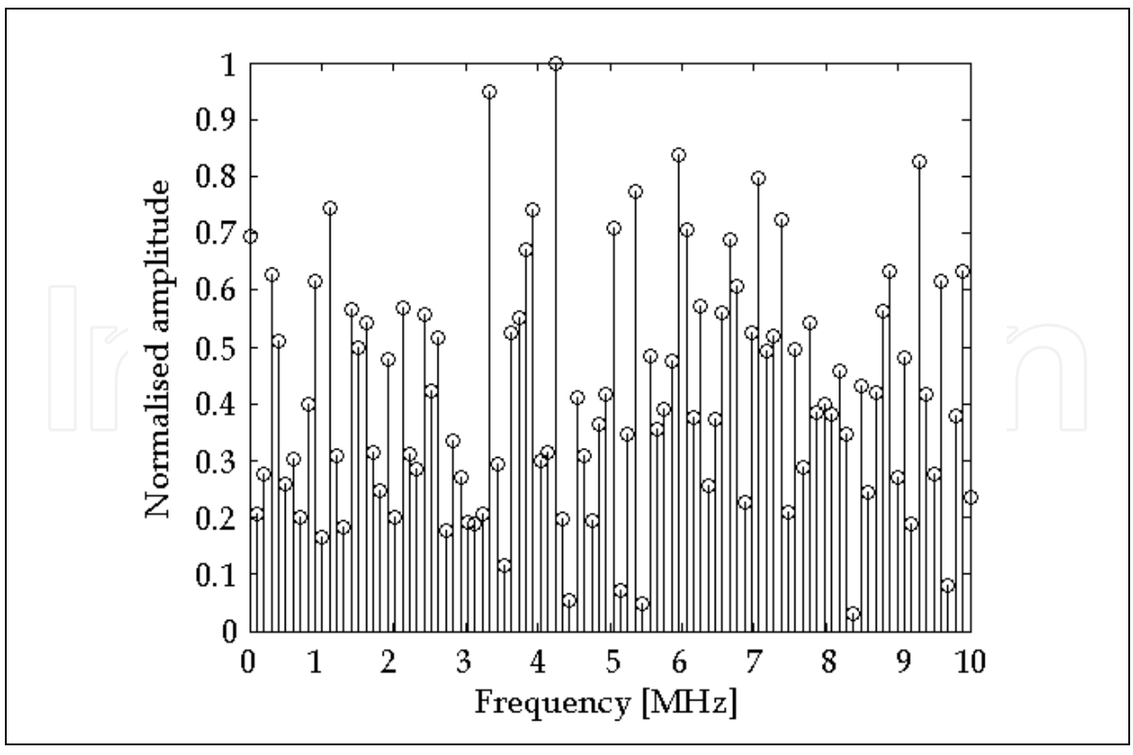

Fig. 17. Normalised frequency (amplitude) spectrum of found excitation $x_2(n)$

Excitation	H_H	H_F	F_F	F_H
$x_1(n)$	0.25	0.75	0.93	0.07
Step	0.03	0.97	0.96	0.04

Table 4. Fault detection efficiency (ad. 2)

	D_1	D_2	D_3	D_4	D_5	D_6	D_7	D_8
F_1	**0.32**	0.02	0.03	0.29	0.03	0	0.27	0
F_2	0.04	**0.36**	0.10	0.01	0	0.05	0	0.17
F_3	0.05	0.23	**0.47**	0	0.04	0	0	0.14
F_4	0.14	0.04	0	**0.43**	0	0.18	0.08	0
F_5	0.01	0	0.14	0	**0.73**	0	0.12	0
F_6	0	0.01	0	0.08	0	**0.71**	0	0.18
F_7	0.17	0	0	0.03	0	0	**0.80**	0
F_8	0	0.19	0.02	0	0	0.05	0	**0.72**

Table 5. Fault location efficiency for specialised excitation (ad. 2)

	D_1	D_2	D_3	D_4	D_5	D_6	D_7	D_8
F_1	**0.14**	0.01	0	0.19	0.29	0.01	0.12	0.22
F_2	0	**0.13**	0.03	0.03	0.37	0.02	0	0.34
F_3	0	0.11	**0.12**	0.04	0.35	0	0	0.34
F_4	0.15	0.02	0	**0.28**	0.20	0.03	0.03	0.21
F_5	0	0	0.06	0.14	**0.41**	0	0.02	0.37
F_6	0.04	0.06	0	0.05	0.21	**0.15**	0	0.37
F_7	0.10	0	0	0.20	0.27	0	**0.27**	0.16
F_8	0	0.21	0.04	0	0.23	0.01	0	**0.49**

Table 6. Fault location efficiency for step excitation (ad. 2)

Found specialised excitation $x_2(n)$ increased test yield in case of fault detection (tab. 4) and, in most cases, increased efficiency of a proper fault location (tab. 5 and 6).

Ad. 3

Figure 18 presents found excitation in time domain and its normalised amplitude spectrum in figure 19. Table 7 shows efficiency of fault detection for step and specialised excitation (probabilities of a healthy circuit correct detection - true positive H_H; healthy circuit incorrect detection – false negative H_F; faulty circuit correct detection - true negative F_F and faulty circuit incorrect detection - false positive F_H). Similar data, but for case of fault location (probabilities of fault F_x classified as D_x, with correct decisions in main diagonal) can be found in tab. 8 for found excitation and tab. 9 for diagnosis with step excitation.

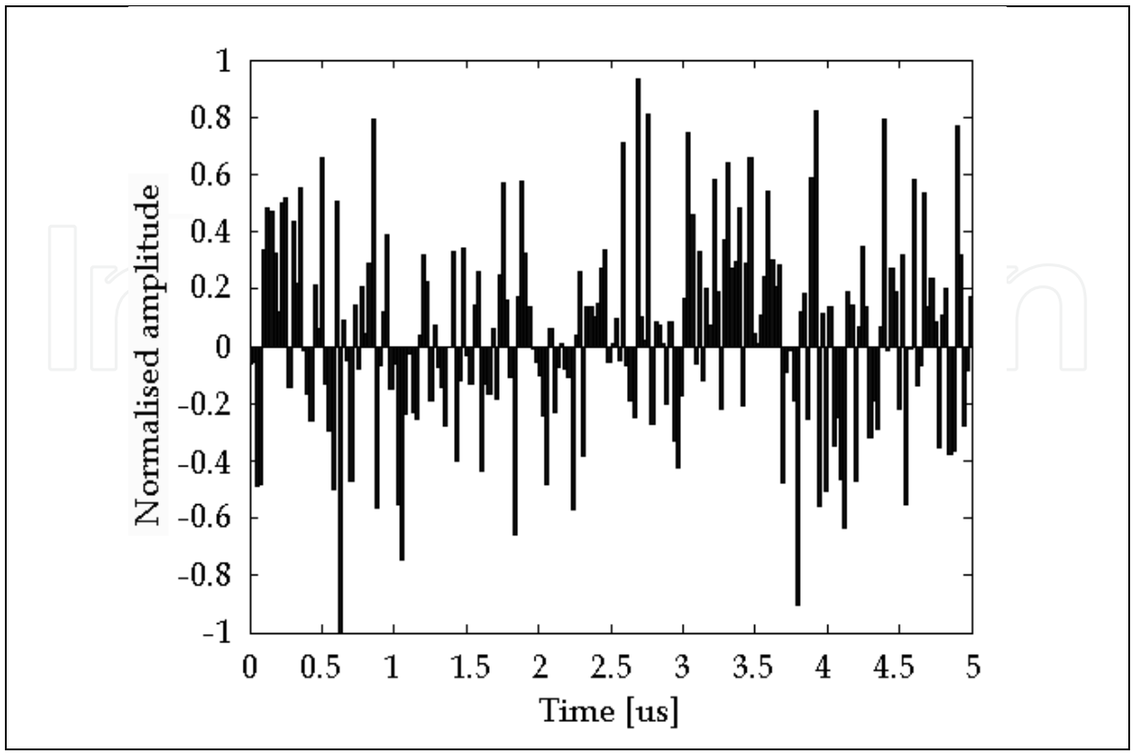

Fig. 18. Found specialised excitation $x_3(n)$

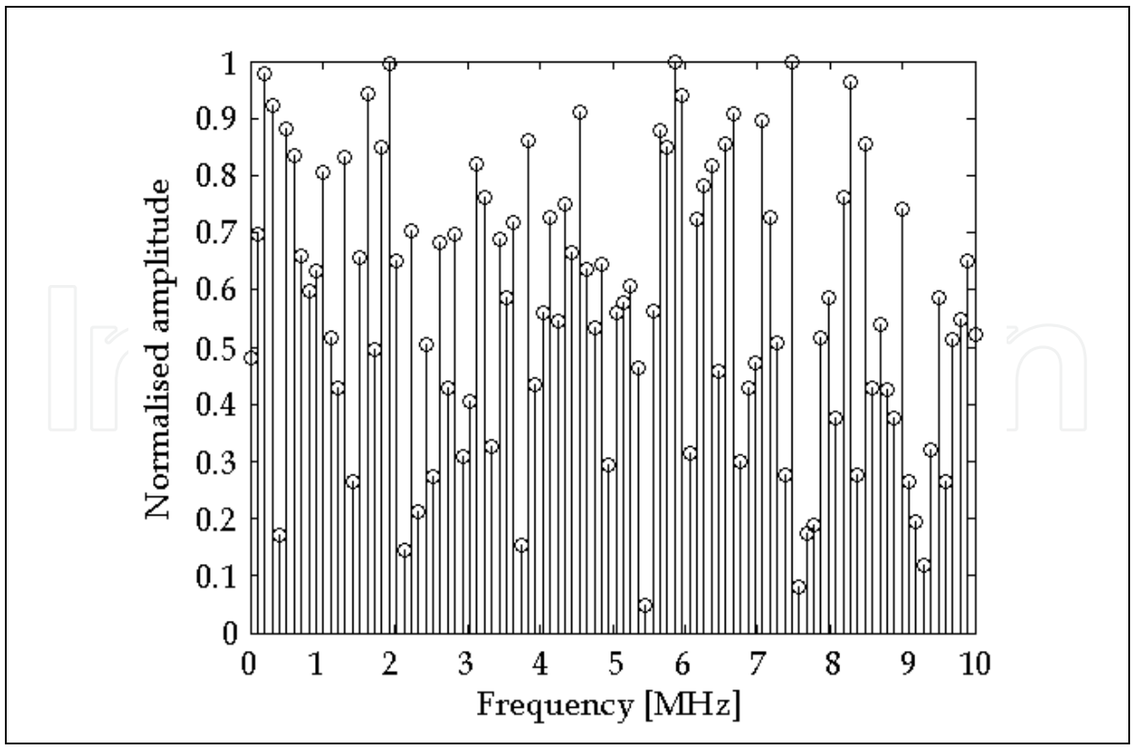

Fig. 19. Normalised frequency (amplitude) spectrum of found excitation $x_3(n)$

Excitation	H_H	H_F	F_F	F_H
$x_3(n)$	**0.17**	0.83	0.90	0.10
Step	**0.16**	0.84	0.91	0.09

Table 7. Fault detection efficiency (ad. 3)

	D_1	D_2	D_3	D_4	D_5	D_6	D_7	D_8
F_1	**0.35**	0	0.10	0.14	0.07	0	0.30	0
F_2	0.01	**0.24**	0.16	0.07	0.01	0.07	0	0.28
F_3	0.04	0.19	**0.20**	0.14	0.02	0.06	0	0.07
F_4	0.33	0.02	0.17	**0.15**	0.05	0.01	0.18	0
F_5	0.32	0	0.18	0.23	**0.11**	0	0.12	0
F_6	0.01	0.15	0.16	0.13	0.03	**0.06**	0	0.31
F_7	0.08	0	0	0	0	0	**0.92**	0
F_8	0	0.17	0	0	0	0.13	0	**0.67**

Table 8. Fault location efficiency for specialised excitation (ad. 3)

	D_1	D_2	D_3	D_4	D_5	D_6	D_7	D_8
F_1	**0.16**	0.02	0.10	0.36	0.04	0.07	0.04	0.10
F_2	0.10	**0**	0.15	0.09	0.02	0.05	0.05	0.45
F_3	0.07	0.02	**0.28**	0.08	0	0.04	0.01	0.40
F_4	0.12	0.01	0.11	**0.37**	0.04	0.02	0.05	0.16
F_5	0.12	0.06	0.19	0.14	**0**	0.06	0.05	0.26
F_6	0.11	0.02	0.25	0.08	0.06	**0.06**	0.02	0.30
F_7	0.24	0.03	0.04	0.52	0.01	0.01	**0.09**	0.01
F_8	0.05	0.03	0.23	0	0.01	0.03	0	**0.57**

Table 9. Fault location efficiency for step excitation (ad. 3)

Designed specialised excitation $x_3(n)$ together with utilisation of wavelet transform has increased efficiency of a proper fault location (tab. 8 and 9), with exception of faults F_3 and F_4. However, it must be noted that specialised excitation together with wavelet transform enabled proper location of faults F_2 and F_5 (tab. 9, marked blue), which cannot be localised at all using simple step excitation.

4.2 Example 2: Active low-pass filter

Figure 20 presents active low-pass filter (Kaminska et al., 1997). Designed excitation x(n) has been approximated by a 0^{th} order polynomial (fig. 4). Amplitude of each sample x_n is binary coded by $N_B = 3$ bits. Width t_w of each interval is changed in range 1 do 8 μs and its resolution is $M_B = 2$ bits coded by Gray code. Non-faulty tolerances were equal 2% for resistors and 5% for capacitors. There were selected 8 parametric (soft) faults of discrete elements (R_1, R_2, R_3 and C): ±10% shift above and below nominal values.

There have been analysed four active CUT responses (fig. 1). Assumed observation windows was T_{max} = 50 μs after last falling edge of the excitation. This value is also equal to time when circuit reaches steady state after step excitation.

There have been investigated two cases:

1. D-Tester (without wavelet transform) and one-dimensional Euclidean distance metrics (11).
2. DW-Tester with *Meyer* base wavelet and two-dimensional Euclidean distance metrics (30).

Fig. 21 and 22 present found excitations for case 1 and 2 respectively. Tab. 10 presents diagnosis efficiency for defined faults and excitations.

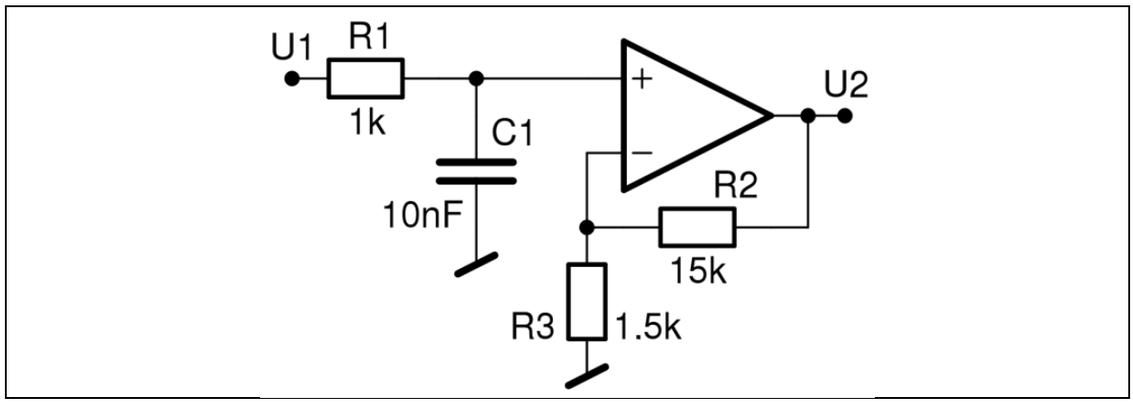

Fig. 20. Active low-pass filter (Kaminska et al., 1997)

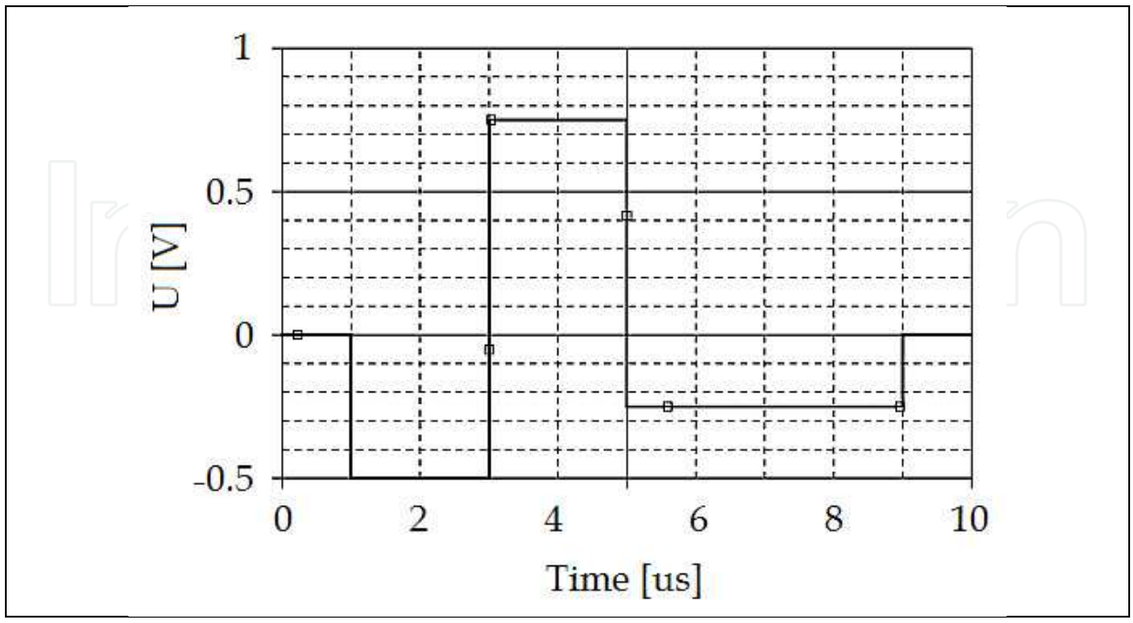

Fig. 21. Found specialised excitation for case 1

Case	Excitation	F_1	F_2	F_3	F_4	F_5	F_6	F_7	F_8
1	$x_1(n)$	0.68	0.63	0.58	0.63	0.74	0.68	1.00	1.00
	Step	0.47	0.42	0.79	0.63	0.37	0.47	0.74	0.89
2	$x_2(n)$	0.58	0.63	0.68	0.47	0.89	0.74	1.00	1.00
	Step	0.58	0.63	0.53	0.63	0.21	0.53	1.00	1.00

Table 10. Fault location efficiency

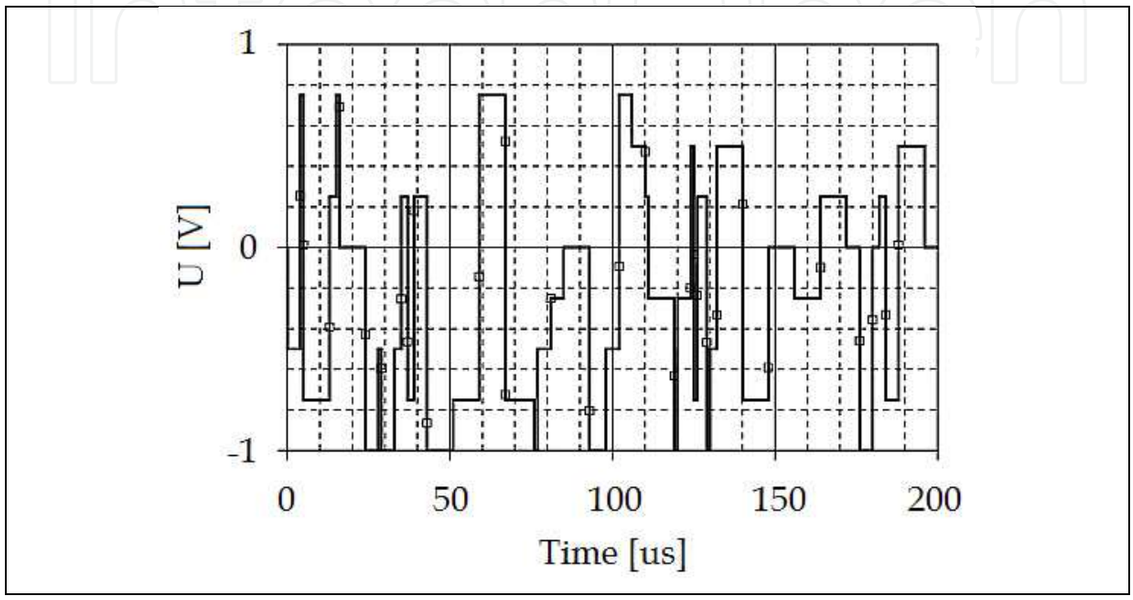

Fig. 22. Found specialised excitation for case 2

Found specialised excitation improved efficiency of analysed single parametric (soft) faults. Utilisation of wavelet transform brought further improvements: i.a. there has been reached 100% proper location of faults F_7 and F_8. Improvement of fault diagnosis was also obtained in testing using simple step excitation (tab. 10, case 2).

5. Conclusions

Utilisation of a wavelet transform as a feature extraction from CUT responses and in building fault dictionary resulted in general improvement of diagnosis efficiency. There have been investigated single catastrophic (hard) and parametric (soft) faults of passive and active analogue electronic circuits. It must be emphasized that the last faults are much more difficult to diagnose, because their influence on circuit behaviour (e.g. transfer function) is much weaker than catastrophic ones. It must be also noted that fault location is more difficult diagnostic goal than fault detection ("just" a differentiation between healthy and faulty circuits). Wavelet transform has been found useful tool in diagnosis of analogue electronic circuits, both in reference cases of simple excitations (step function, real Dirac pulse, linear function) and in cases when excitation has been designed by genetic algorithm. In every case, combination of specialised excitation and wavelet transform resulted in highest efficiency of fault diagnosis.

It has been also found that in some cases (example 2) utilisation of wavelet transform allowed 100% location of a selected faults. Merging genetic algorithm and wavelet transform in example 1 allowed design of test excitation which enabled location of faults completely hidden for diagnosis using step excitation.

It must be also added that abovementioned results have been achieved for simple, non-optimised classifiers based on simple, the closest neighbourhood metrics.

6. References

Baker K., Richardson A. M., Dorey A. P., *Mixed signal test techniques, applications and demands*, IEEE Circuits, Devices, Systems, 1996, vol. 146, pp. 358-365

Balivada A., Chen J., Abraham J. A., *Analog testing with time response parameters*, IEEE Design and Test of Computers, 1996, vol. 13, pp. 18-25

Bernier J. L., Merelo J. J., Ortega J., Prieto A., *Test Pattern Generation for Analog Circuits Using Neural Networks and Evolutive Algorithms*, International Workshop on Artificial Neural Networks, 1995, vol. s. 838–844

Chruszczyk L., Rutkowski J., Grzechca D., *Finding of optimal excitation signal for testing of analog electronic circuits*, International Conference on Signals and Electronic Systems, 2006, Łódź, Poland, pp. 613–616

Chruszczyk L., Grzechca D., Rutkowski J., „Finding of optimal excitation signal for testing of analog electronic circuits", Bulletin of Polish Academy of Sciences, September 2007, pp. 273–280

Chruszczyk L., Rutkowski J., *Excitation optimization in fault diagnosis of analog electronic circuits*, 11th IEEE Workshop on Design and Diagnostics of Electronic Circuits and Systems, 2008, Bratislava, Slovak Republic, pp. 1–4

Chruszczyk L., Rutkowski J., *Optimal excitation in fault diagnosis of analog electronic circuits*, IEEE International Conference on Electronics, Circuits and Systems, 2008, Malta

Chruszczyk L., Rutkowski J., *Specialised excitation and wavelet transform in fault diagnosis of analogue electronic circuits*, IInd International Interdisciplinary Technical Conference of Young Scientists, 2009, Poznan, Poland

Chruszczyk L., *Fault diagnosis of analog electronic circuits with tolerances in mind*, 18th International Conference Mixed Design of Integrated Circuits and Systems, 2011, Gliwice, Poland, *book of abstracts* p. 126. Reprinted in Elektronika № 11/2011 (*in press*), monthly magazine of Association of Polish Electrical Engineers (SEP)

Chruszczyk L., *Tolerance Maximisation in Fault Diagnosis of Analogue Electronic Circuits*, 20th European Conference on Circuit Theory and Design, 2011, Linkoping, Sweden, pp. 914–917

Chruszczyk L., Rutkowski J., *Tolerance Maximisation in Fault Diagnosis of Analogue Electronic Circuits*, Electrical Review № 10/2011 (The Magazine of Polish Electricians), Poland, p. 159

Dai H., Souders M., *Time domain testing strategies and fault diagnosis for analog systems*, 1989, IEEE Instrumentation and Measurement Technology Conference, pp. 293–298

Daubechies I., „Ten lectures on wavelets", CBMS, SIAM, 1992

De Jong K. A., „An analysis of the behavior of a class of genetic adaptive systems", (PhD thesis), 1975, University of Michigan, USA

De Jong K. A., „Adaptive system design. A genetic approach.", IEEE Transactions on Systems, Man and Cybernetics, SMC-10(9), 1980, pp. 566–574

Goldberg D. E., „Genetic Algorithms in Search, Optimization & Machine Learning", Addison-Wesley, 1989

Grefenstette J. J., „Parallel adaptive algorithms for function optimization", 1981, Vanderbilt Univ., Nashville, USA

Grefenstette J., J., *Optimization of Control Parameters for Genetic Algorithms*, IEEE Transactions on Systems, Man and Cybernetics, 1986, vol. 16, pp. 122–128

Holland J. H., „A new kind of turnpike theorem", Bulletin of the American Mathematical Society, 1968, 75, 1311–1317

Huertas J. L., *Test and design for testability of analog and mixed-signal IC: theoretical basic and pragmatical approaches*, European Conference On Circuit Theory And Design, Davos, Switzerland, 1993, pp. 75–156

Kaminska, B. et al., *Analog and mixed-signal benchmark circuits - first release*, IEEE International Test Conference, Washington, USA, 1997

Kilic Y., Zwolinski M., *Testing analog circuits by supply voltage variation and supply current monitoring,* IEEE Custom Integrated Circuits, 1999, pp. 155–158

Milne A., Taylor D., Naylor K., *Assesing and comparing fault coverage when testing analogue circuits*, 1997, IEE Circuits Devices Systems, vol. 144

Milor L., Sangiovanni-Vincentelli A. L., *Minimizing production test time to detect faults in analog circuits*, IEEE CAD of Integrated CAS, 1994, vol. 13, pp. 796–813

Pecenka T., Sekanina L., Kotasek Z., *Evolution of synthetic RTL benchmark circuits with predefined testability*, ACM Transactions on Design Automation of Electronic Systems (TODAES), 2008, vol. 13, ed. 3, art. No. 54

Pettey C. B., Leuze M. R., Grefenstette J. J., *A parallel genetic algorithm*, IInd International Conference on Genetic Algorithms, 1987, pp. 155–161

Saab K., Hamida N.B., Kamińska B., *Closing the Gap Between Analog and Digital Testing*, IEEE Trans. Computer-Aided Design, vol. 20, No. 2, pp. 307–314, 2001

Savir J., Guo Z., *Test Limitations of Parametric Faults In Analog Circuits*, IEEE Trans. on Instrumentation and Measurement, vol. 52, no. 5, October 2003

Somayajula S. S., Sanchez-Sinecio E., Pineda de Gyvez J., *Analog Fault Diagnosis Based on Ramping Power Supply Current Signature Clusters*, 1996, IEEE Circuits and Systems, vol. 43, No. 10, pp. 703

Suh J. Y., Van Gucht D., *Incorporating heuristic information into genetic search*, IInd International Conference on Genetic Algorithms, 1987, pp. 100–107

Tanese R., *Parallel genetic algorithms for a hypercube*, IInd International Conference on Genetic Algorithms, 1987, pp. 177–183

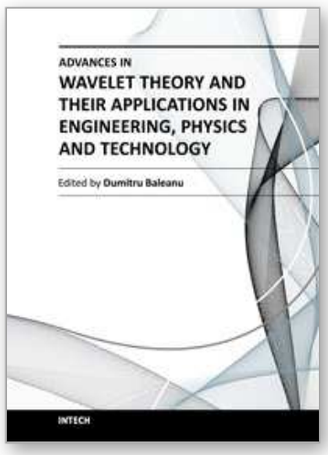

Advances in Wavelet Theory and Their Applications in Engineering, Physics and Technology

Edited by Dr. Dumitru Baleanu

ISBN 978-953-51-0494-0
Hard cover, 634 pages
Publisher InTech
Published online 04, April, 2012
Published in print edition April, 2012

The use of the wavelet transform to analyze the behaviour of the complex systems from various fields started to be widely recognized and applied successfully during the last few decades. In this book some advances in wavelet theory and their applications in engineering, physics and technology are presented. The applications were carefully selected and grouped in five main sections - Signal Processing, Electrical Systems, Fault Diagnosis and Monitoring, Image Processing and Applications in Engineering. One of the key features of this book is that the wavelet concepts have been described from a point of view that is familiar to researchers from various branches of science and engineering. The content of the book is accessible to a large number of readers.

INTECH
open science | open minds

InTech Europe
University Campus STeP Ri
Slavka Krautzeka 83/A
51000 Rijeka, Croatia
Phone: +385 (51) 770 447
Fax: +385 (51) 686 166
www.intechopen.com

InTech China
Unit 405, Office Block, Hotel Equatorial Shanghai
No.65, Yan An Road (West), Shanghai, 200040, China
中国上海市延安西路65号上海国际贵都大饭店办公楼405单元
Phone: +86-21-62489820
Fax: +86-21-62489821

IntechOpen